Experiments in Fluids 26 (1999) 470–474 © Springer-Verlag 1999

# Electrical measurement of sediment layer thickness under suspension flows

**F. de Rooij, S. B. Dalziel, P. F. Linden**



**Abstract** This paper reports a new technique to measure the thickness of a layer of deposited sediment as a function of time, independent of the flow conditions or presence of suspended sediment above the layer. Small electrodes on the bottom and a reference electrode in the fluid above were used to measure the resistance of the layer with a small *AC* current and a bridge circuit. Using a multiplexer and an Analog-to-Digital converter the growth of the layer can be accurately monitored at many locations on the tank bottom. In a trial experiment the sedimentation under a stagnant column of a monodisperse suspension was examined. The results show that changes in the sediment layer thickness of less than 0.3% can be measured for layers up to 0.2 g/cm$^2$.

## 1 Introduction

The sedimentation of suspended material plays an important role in many geophysical and industrial flows. The sedimentation from turbidity currents, arising in the oceans from underwater landslides, is of great interest to geologists (see Middleton 1993 and references therein). Improved understanding of how rock layers are produced by these turbidity currents allows them to predict more accurately where oil reservoirs might have formed. In the atmosphere, volcanic ash clouds may transport ash many thousands of kilometres before it sediments out to the Earth's surface (Holasek et al. 1996). A striking example was the recent Pinatubo eruption. An industrial application of sedimentation can be found in wastewater treatment plants. The treatment process usually includes both a primary sedimentation tank where the solid material sediments out of the flow, and, after the biological treatment, a secondary sedimentation tank where the formed organic flocs sediment out (Ashley 1996).

*Received*: *8 February 1998*/*Accepted*: *19 July 1998*

F. de Rooij, S. B. Dalziel, P. F. Linden
Department of Applied Mathematics and Theoretical Physics
University of Cambridge, Silver Street
Cambridge CB3 9EW, UK

*Correspondence to*: F. de Rooij

We thank David Lipman for his technical assistance in the designing and building of the experimental apparatus. The financial support for this work from Yorkshire Water is gratefully acknowledged.

Although the sedimentation from a dilute suspension of monodisperse particulate in a stationary ambient is well understood, many aspects of sedimentation are still subject of current research. Effects that introduce complications include bottom topography, bounded domains, ambient flow, background rotation, stratification, high particle concentrations and polydisperse particulate. These flows are often hard to capture with computational methods, and frequently laboratory experiments are carried out to obtain a deeper understanding of the flow (see e.g. Ernst et al. 1996; Bennett and Bridge 1995; Bonnecaze et al. 1993, and earlier papers referred to by Middleton 1993). For these experiments it is desirable to have a technique to measure the thickness of the layer of sediment that accumulates on the bottom of the tank. Several experimental techniques have been described in the literature. Both Bonnecaze et al. (1993) and Garcia (1994) used a "vacuuming" method, in which they siphon up the particles deposited on a known area at several locations in the tank, dry the samples, and determine the weight of the samples with a scale. The accuracy is indicated by the integrated deposition which is within 5% of the total released mass (Bonnecaze et al. 1993). Best and Ashworth (1994) describe the use of an ultrasonic depth probe, a technique which has recently been extended by mounting the probe on a precision horizontal traverse system on top of the experimental tank. McCaffrey (1997) reports a vertical resolution of 10 μm for this ultrasonic bed profiler. Although this system offers a detailed spatial resolution, measurements can only be taken after all the particles have sedimented out. Suspended particles affect the sound speed and thus the accuracy of the measurements.

The present paper describes a new method to measure the local sediment layer thickness. Although the spatial resolution is limited, it allows the measurement of the time-evolution of the thickness, irrespective of the ambient flow conditions. In Section 2 we describe the experimental apparatus, and in Section 3 we describe the calibration and the theory underlying it. Section 4 gives the results of a trial experiment, and the conclusions are given in Section 5.

## 2 Apparatus

Our technique is based on the fact that the electrical resistance of a layer of particles depends on the thickness of the layer. In our experiments we use fine Silicon Carbide particles, normally used as industrial grinding powder. These black particles have a density of 3.217 g/cm$^3$ and have an irregular angular shape (see Fig. 1 in Huppert et al. 1991). In the

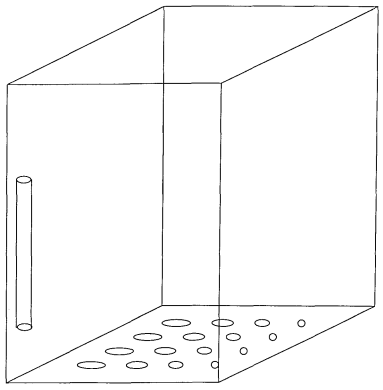

**Fig. 1.** Sketch of the experimental tank with locations of the electrodes

experiments reported here we use particles with a median equivalent diameter of 13 μm, and a slightly right-skewed size distribution: 3% (by volume) of the particles are smaller than 5 μm, and 6% are larger than 25 μm. The electrical resistance of this material is much higher than that of tap water, so the water conducts the current when a voltage is applied, and only when a large volume fraction is occupied by particles is the resistance increased and the current reduced. These high volume fractions are achieved in the sediment layer that accumulates on the bottom in sedimentation experiments. The thickness of the layer can thus be determined by measuring its resistance. It is important to note here that the particle size and shape affect the packing density, and therefore the resistance of the layer. The apparatus will thus have to be calibrated for the specific geometry of the particles used. Also, the particle size distribution needs to be fairly narrow, in order to avoid spatial or temporal variations in the sizes of the sedimenting particles and different packing arrangements forming in the sedimented layer.

We measure the resistance of the sediment layer with an electrode in the fluid above the layer and electrodes on the tank bottom below the layer (see Fig. 1). The position of the top electrode is relatively unimportant, since the resistance of the fluid is much lower than the resistance of a sediment layer, and there is a concentration of field lines near the bottom electrodes. In the experimental apparatus a stainless steel rod, 8.0 cm long and 0.60 cm diameter, mounted vertically in a corner at 1.5 cm above the bottom, was used as a reference electrode for all measurements. The size of the bottom electrodes determines the range of layer thicknesses that can be measured, as discussed in Section 3. For the experiments we used a rectangular Perspex tank with inside dimensions $19.0 \times 20.0 \times 25.0$ cm$^3$ ($l \times b \times h$). The bottom plate contained a total of 16 circular disks as bottom electrodes, with four different sizes: 1, 2, 4 and 6 mm diameter. The stainless steel electrodes were screwed into holes in the plate, on a rectangular grid with a spacing of 5.0 cm. The tops of the electrodes were machined flush with the bottom of the tank. During the design of the experimental equipment we also considered other electrode configurations, such as long rectangular strips. These could yield an averaging of the sediment thickness along their length, but this option was discarded since a very small area without sediment has a disproportionately strong effect due to the nonlinear averaging of the electric field.

To measure the small changes in the resistance accurately, the electrodes were connected to a bridge circuit, the basic function of which is depicted schematically in Fig. 2. One of the resistors in the bridge, indicated by $R_s$, was switched to one of six values in the range from 1 to 50 kΩ, to match the resistance $R_e$ between the electrodes reasonably closely. To avoid electrolysis of the water, an *AC* electrical source with a frequency of 2.2 kHz was used. The output from the bridge circuit was amplified, rectified and filtered to produce a fluctuating *DC* voltage. The characteristic time of the filtering was approximately 5 ms, corresponding to 11 cycles of the *AC* source signal. The signal output of the rectifier was monitored with an oscilloscope to detect clipping of the bridge circuit, which occurred at about 3.2 V. The resistance $R_s$ was selected to achieve the maximal signal output without clipping.

The output of the low pass filter was connected to an analog-to-digital converter (*ADC*) on a data acquisition board (DT-2812) in a PC. The accuracy of this *ADC* is twelve bits, or 1/4096, and the sampling time is 16.7 μs. A 256-channel multiplexer was purpose-built to allow fast switching of the bridge circuit between the different bottom electrodes. The multiplexer design includes two tiers of semiconductor 16-channel analog multiplexers (MAX-396), with a typical switching time of 0.1 μs. The data acquisition board was also used to produce the digital data lines that control the multiplexer. A software module was written to allow easy logging of multiplexed data series, and incorporated into the DigImage software package (Dalziel 1992). Note that the characteristic time of the filtering limits the maximum sampling rate, since the characteristic times of both the multiplexer and the *ADC* are much shorter.

## 3 Calibration

Before calibrating the apparatus for our specific particle size, we checked the assumptions given in Section 2 on which the design was based. First we checked whether the resistance $R_e$

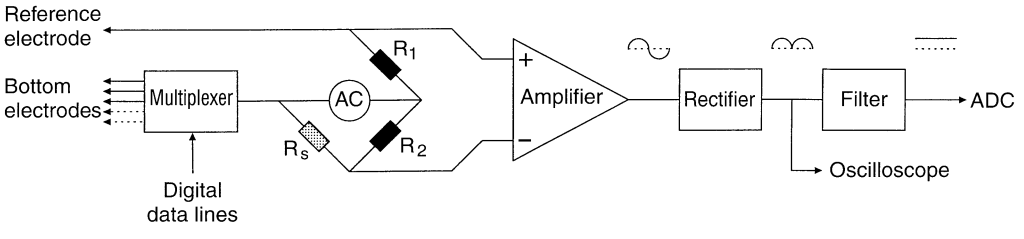


**Fig. 2.** Diagram of the bridge circuit and connections

between the reference electrode and the bottom electrodes depends on the ambient fluid properties. Starting from a tank filled with just tap water, the *ADC* reading remained unchanged after addition of half a teaspoon of wetting agent. (The wetting agent is needed to facilitate suspending particles in the fluid.) The *ADC* reading still remained unchanged after suspending up to 20 kg/m$^3$ Silicon Carbide particles in the fluid. This shows that the ambient suspension concentration does not affect the resistance between the electrodes. Adding salt to the fluid, however, changes the resistance substantially. Experiments investigating the combined effects of particulate and salinity gradients would require an independent measure of the conductivity of the saline fluid near the bottom.



Next, we investigated whether the resistance $R_e$ depends on the positioning of the electrodes. The *ADC* reading was found to be independent of the distance between the reference electrode and the bottom electrodes. Measurements of the resistance between different bottom electrodes were also independent of the spacing between the electrodes. However, these checks did indicate that the size of the electrodes is important for the resistance. As expected, larger bottom electrodes yield a lower resistance. The reference electrode has to be completely submersed, because otherwise fluctuations in fluid surface level will affect the *ADC* readings.

The fact that neither the ambient fluid properties, nor the electrode spacing has a measurable effect on $R_e$ leads us to the assumption that $R_e$ is the sum of a constant resistance $R_c$ and the resistance of the layer $R_{\text{layer}}$, which we can calculate from the electrical field lines through the layer in the immediate vicinity of the bottom electrode. To obtain an equation with which we model the calibration data, we simplify the configuration of the field lines for the calculation and assume that they are straight and lie on conical surfaces, as depicted in Fig. 3. We also assume that all field lines originate at a virtual origin at a distance $a$ below the middle of the electrode, which has a radius $r$, which determines the smallest angle $\alpha$ between field lines and the horizontal plane.

To calculate the resistance of the layer, which has a resistivity $\rho_e$, we integrate the resistance of the cone from $z=a$ to $z=a+d$:

$$R_{\text{layer}} = \int_a^{d+a} \frac{\rho_e}{A(z)}\,\mathrm{d}z \tag{1}$$

where $A(z)$ denotes the cross-sectional area of the cone: $A(z)=\pi r^2(z/a)^2$. Substituting this into Eq. (1) and integrating yields

$$R_{\text{layer}} = \frac{\rho_e d}{\pi r^2}\left(1+\frac{d}{r\tan\alpha}\right)^{-1} \tag{2}$$

The output $V(d)$ of the bridge circuit is inversely proportional to the resistance $R_e = R_{\text{layer}} + R_c$,

$$V = \frac{C}{R_{\text{layer}}+R_c} \tag{3}$$

where $C$ is a constant of proportionality with the units of current. Combining Eqs. (2) and (3) gives the layer thickness

$$d = \frac{\pi r^2}{\rho_e}\left(\frac{C}{V}-R_c\right)\left[1-\frac{\pi r}{\rho_e\tan\alpha}\left(\frac{C}{V}-R_c\right)\right]^{-1} \tag{4}$$

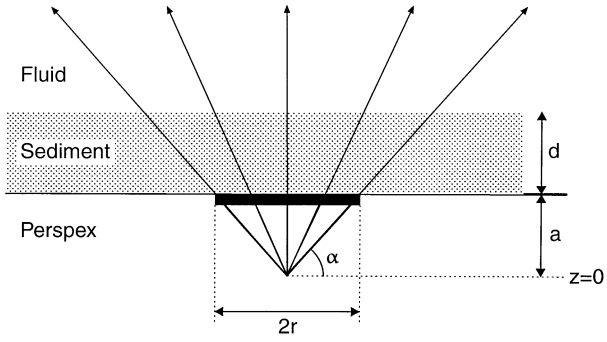


**Fig. 3.** Electrical field lines through the sediment layer above a bottom electrode

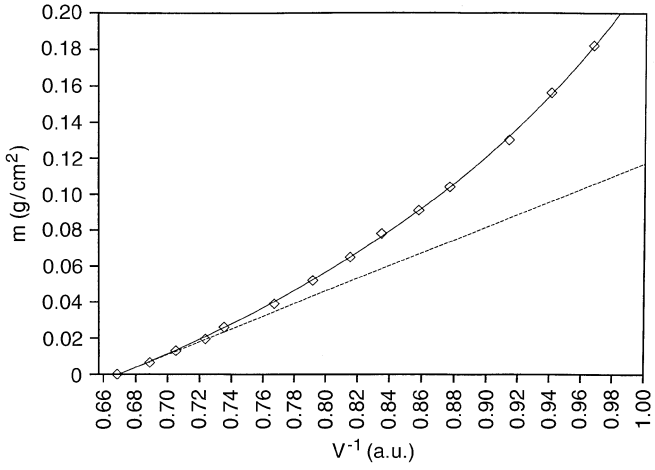


**Fig. 4.** Calibration of sediment mass per area against output voltage, for a bottom electrode with 4 mm diameter. The dashed line is a linear fit to the data for thin layers, and the solid calibration curve is obtained by fitting the third constant $C_3$ to the ratios of the residues

The layer thickness $d$ is proportional to the sediment mass per unit area $m$, and we can write

$$m = \frac{C_1+\dfrac{C_2}{V}}{1-C_3\left[C_1+\dfrac{C_2}{V}\right]} \tag{5}$$

where the constants $C_1$, $C_2$ and $C_3$ are related through the bulk density of the (dry) sediment to $-\pi r^2 R_c/\rho_e$, $\pi r^2 C/\rho_e$ and $(r\tan\alpha)^{-1}$, respectively. In practice we determine these constants experimentally for each electrode, sediment type and bridge setting $R_s$. The numerator, $m_{\text{lin}} = C_1 + C_2/V$ provides a linear approximation for $m$ which is valid for thin layers of sediment $d \ll r$.

To calibrate the apparatus we need values for the constants in Eq. (5). Carefully weighed amounts of particles were added to the fluid in the tank and the fluid was thoroughly stirred to obtain a homogeneous suspension. The stirring was stopped and the particles were allowed to settle, and we assume this created a sediment layer of homogeneous thickness on the tank floor. When visual observation indicated that all particles had settled, the bridge output $V$ was measured. Fig. 4 shows a graph of the mass per unit area versus $1/V$ for a typical data set.

A least-squares fit to the first few data points yielded the constants $C_1$ and $C_2$ of the linear approximation $m_{lin}$, indicated with a straight line in Fig. 4. To obtain the constant $C_3$ for the nonlinear deviation from this linear approximation, a curve was fitted to $m/m_{lin}$ plotted against $m_{lin}$, forced to go through 1 at $m_{lin}=0$. The resulting calibration curve is also shown in Fig. 4, and it can be seen to reflect the measurements very well.

## 4 Results

We now use the calibration curves obtained as described in the previous section to measure the growing layer of sediment in a simple trial experiment: a stagnant column of a suspension. The experimental tank was filled with water to a depth $H$ of 10.2 cm, and a carefully weighed amount of particles was added, as well as a few drops of wetting agent. The suspension was thoroughly stirred. Starting at the moment the stirring was stopped, the growth of the sediment layer was monitored over a 10 min period by sampling the output voltage $V$ for each of the 16 bottom electrodes every 5 s. The results are shown in Fig. 5. Time, plotted on the horizontal axis, is non-dimensionalized with the time it would take a spherical particle of the nominal particle size to fall from top to bottom at the Stokes settling velocity, and layer thickness, on the vertical axis, is non-dimensionalised with the final layer thickness. The measurements from different electrode sizes are seen to be in very good agreement with each other. The fluctuation in the measurements with the smallest electrode is approximately 3%. Fluctuations for the larger electrode sizes are less than 1%, comparable with the discretisation error of the *ADC*. The reduced scatter for larger electrodes results from the larger number of particles settling onto the electrode surface.

The initial growth of the layer thickness is seen to be approximately linear, but the growth rate subsequently slowly reduces and the layer thickness asymptotes to its final value. The changing layer growth rate indicates that the suspension was not perfectly monodisperse. If we neglect the initial turbulence resulting from the stirring and any hindrance effects, each particle size $d$ will settle at its own settling velocity $V_s(d)$ until all particles of that size will have reached the bottom of the tank at time $t=V_s/H$. This allows us to calculate the particle size distribution $P(d)$ from the growth of the layer thickness, expressed as the mass per unit area $m(t)$:

$$P(d)=\frac{-2H^2}{V_s^2 d}\left[\frac{\partial^2(m/m_{tot})}{\partial t^2}\right]_{t=H/V_s} \tag{6}$$

The particle size distribution curve calculated using Eq. (6) by differentiating the deposition measurements is shown in Fig. 6. The data for small particle sizes are unreliable, due to the very small changes in the layer growth at later times: the second derivative in Eq. (6) tends to amplify small experimental errors. The shape of the size distribution for sizes larger than 15 μm suggests a good match with the upper bound specified by the manufacturer, although the peak indicates a somewhat higher median size. These results suggest that application of this technique to settling experiments in a taller tank with a more controlled stirring mechanism could yield reliable size distribution measurements.

The growth rate of the layer thickness in the initial phase, expressed as the corresponding settling velocity, is plotted in Fig. 7 for different particle concentrations. We observe a slight decrease of the growth rate with increasing particle concentration. This may be a result of hindered settling occurring close to the bottom of the tank at the higher particle concentrations, reducing the rate at which particles join the closely packed layer that gives the increased electrical resistance. For initial particle volume concentrations above 0.3% the sediment layer grows at a speed of 0.056 cm/s, whereas the Stokes settling velocity for spherical particles with a diameter of 13 μm and a density of 3.217 g/cm$^3$ is 0.020 cm/s. This indicates that a rather large fraction of the particles has an equivalent diameter greater than 13 μm, as also indicated by the particle size distribution shown in Fig. 6.



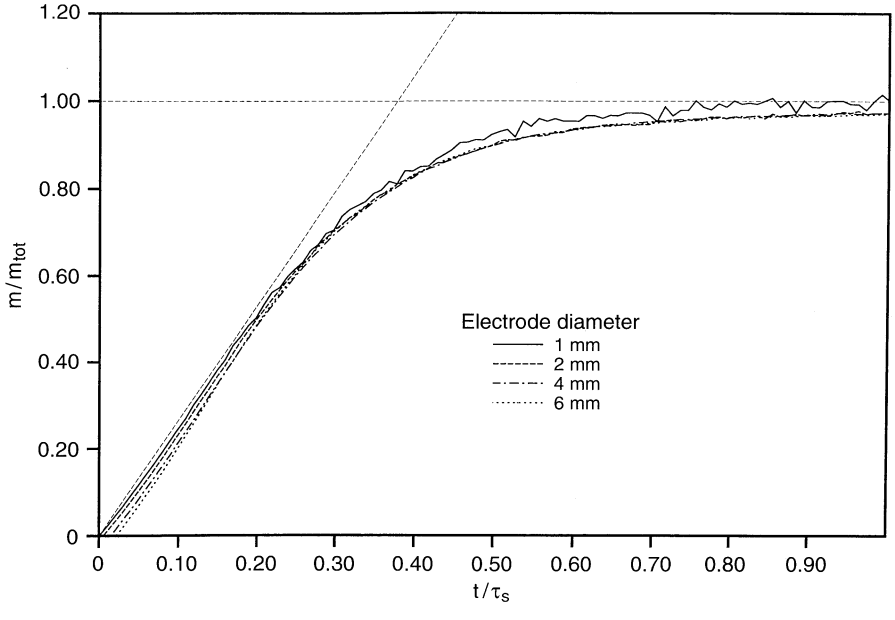


**Fig. 5.** Evolution of the thickness of a sediment layer under a 10.2 cm high stagnant column. The total suspended mass was 70 g and the surface area 0.0380 m$^2$. Each of the four curves represents the average of the four measurements with bottom electrodes of equal diameter, non-dimensionalized with the total suspended mass per unit area. Time is non-dimensionalised with the Stokes settling time $\tau_s=H/V_s$

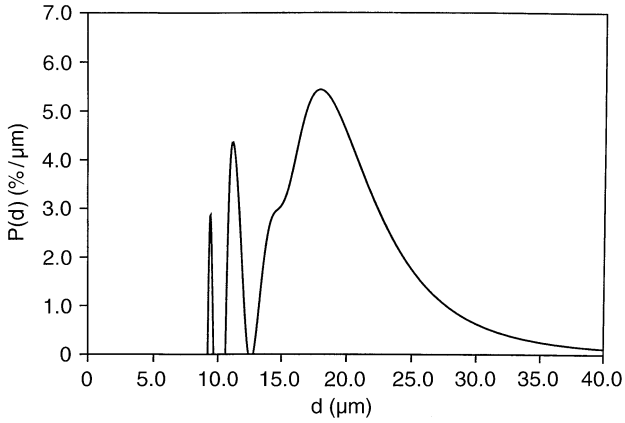


**Fig. 6.** Particle size distribution, calculated from a running 2 min average of the layer thickness growth as measured with the 4 mm electrodes

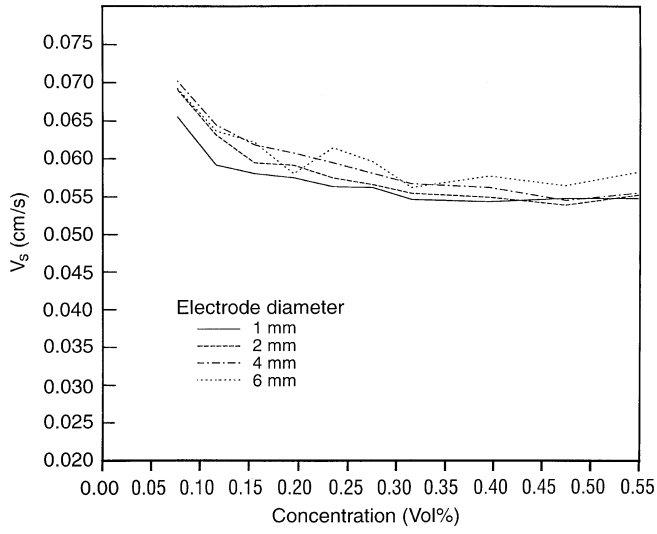


**Fig. 7.** Initial layer thickness growth versus particle volume concentration. Measurements are averaged over 4 electrodes of equal size

## 5 Conclusions

The depositometer described in this paper has been shown to yield very accurate time-dependent measurements of the mass thickness of a layer of sediment. The measurement error in the absolute mass per unit area of the layer is less than 3% for a bottom electrode size of 1 mm. The error is less than 1% for larger electrodes. Changes in the layer thickness can even be measured to the accuracy of the *ADC*. In the present arrangement changes as small as 0.5 mg/cm$^2$ could be measured with the 6 mm electrodes, for layers with a mass of 0.2 g/cm$^2$. Because of their higher accuracy over a larger measurable thickness range, the electrodes of 4–6 mm diameter are considered particularly useful for further experimental measurements. Electrodes larger than that would probably average over a too large an area.

At the moment, the application of this novel technique is limited to flows with no temperature or salinity differences, and to particles with a fairly narrow size distribution. The apparatus has to be calibrated for the specific particles used. However, since the technique yields accurate, non-intrusive and time-resolved measurements, it is a useful tool for a wide range of laboratory investigations of particle-driven flows, in fields such as geophysics, oceanography and engineering. We are currently implementing this technique in a much larger experimental arrangement in order to measure the sedimentation from particle-laden currents.

## References

**Ashley R (ed.)** (1996) Sewer solids – characteristics, movement, effects and control. Proc IAWQ Specialized conf, Dundee, Scotland. Water Science and Technology 33: 9

**Bennett SJ; Bridge JS** (1995) An experimental study of flow, bedload transport and topography under conditions of erosion and deposition and comparison with theoretical models. Sedimentol 42: 117–146

**Best J; Ashworth P** (1994) A high-resolution ultrasonic bed profiler for use in laboratory flumes. J Sedimentary Res A 64: 674–675

**Bonnecaze RT; Huppert HE; Lister JR** (1993) Particle-driven gravity currents. J Fluid Mech 250: 339–369

**Dalziel SB** (1992) DigImage system overview. Cambridge Environmental Research Consultants

**Ernst GGJ; Sparks RSJ; Carey SN; Bursik MI** (1996) Sedimentation from turbulent jets and plumes. J Geophys Res 101: 5575–5589

**Garcia M** (1994) Depositional turbidity currents laden with poorly sorted sediment. J Hydr Eng 120: 1240–1263

**Holasek RE; Woods AW; Self S** (1996) Experiments on gas-ash separation processes in volcanic umbrella plumes. J Volcanol Geotherm Res 70: 169–181

**Huppert HE; Kerr RC; Lister JR; Turner JS** (1991) Convection and particle entrainment driven by differential sedimentation. J Fluid Mech 226: 349–369

**McCaffrey W** (1997) Personal communication

**Middleton GV** (1993) Sediment deposition from turbidity currents. Annu Rev Earth Planet Sci 21: 89–114